

# Observational Impact of Scattered Light from the Laser Beam of a Laser Guide Star Adaptive Optics System

Y. HAYANO AND M. IYE

National Astronomical Observatory of Japan, Mitaka, Tokyo, 181-8588, Japan; y.hayano@nao.ac.jp, iye@optik.mtk.nao.ac.jp

H. TAKAMI AND N. TAKATO

Subaru Telescope, National Astronomical Observatory of Japan, 650 North A'ohoku Place, Hilo, HI 96720; takami@naoj.org, takato@naoj.org

W. GAESSLER

Max-Planck-Institut für Astronomie, Königstuhl 17, D69117 Heidelberg, Germany; gaessler@mpia.de

Y. MINOWA<sup>1</sup>

Department of Astronomy, School of Science, the University of Tokyo, 7-3-1 Hongo, Bunkyo-ku, Tokyo 113-0033, Japan; minoways@naoj.org

AND

P. WIZINOWICH AND D. SUMMERS

Keck Observatory, 65-1120 Mamalahoa Highway, Kamuela, HI 96743; peterw@keck.hawaii.edu, dsummers@keck.hawaii.edu

*Received 2003 June 5; accepted 2003 September 16*

**ABSTRACT.** The scattered light from the sodium laser beam projected from the Keck II telescope during their laser guide star experiment campaign conducted at the end of 2001 was measured using the Subaru Telescope, 221 m away from the Keck II telescope. The purpose of our measurement was to evaluate the observational impact of the scattered light from the laser beam on other telescopes whose field of view happens to cross the laser beam. The actual flux level at the wavelength of 589 nm (sodium D2 line) measured when the Subaru Telescope was pointing toward the Keck II laser beam at elevation angles of 45° and 60° was roughly equivalent to 19.5 mag arcsec<sup>-2</sup> calibrated by a standard-star magnitude in the *R* band. The present measurements provide the first quantitative assessment of the level of scattered light from the laser beam observed from other nearby telescopes. The results of measurements were shown to be consistent with theoretical estimation based on the laser beam flux and the efficiency of the scattering due to molecules and aerosols in the atmosphere. Although the impact of this scattered light depends on the type of observation, we show that the surface brightness of the sodium laser beam at the focal plane of the telescope is no brighter than the sky background 45° away from the full moon, when the collision of the laser beam and telescope pointing takes place at relatively low altitude, for instance several hundred meters above the ground. In this case, many observations could be performed without significant deterioration. Disturbance to astronomical observations could be significant, however, when a nearby telescope is pointed in the vicinity of the laser guide star, because of the presence of the defocused laser guide star itself at around 10 mag in the observing field of view, or because of the increase of total flux of scattered light from the laser beam that occurs when the optical axis of the telescope and the center of the laser beam collide at an altitude of around 8 km.

## 1. INTRODUCTION

A laser guide star system provides an artificial light source to measure the atmospheric turbulence along the line of sight to any astronomical target and dramatically increases the usefulness of the adaptive optics (AO) system by increasing its sky coverage without the need of bright natural guide stars. The sodium laser guide star at the wavelength of 589 nm (sodium D2 line) is one

of the key technologies to enhance the observing capability of existing 8–10 m class telescopes (Wizinowich et al. 1998b; Bonaccini et al. 2002; D'Orgeville et al. 2002; Hayano et al. 2003) and for the planned next generation of extremely large telescopes (Le Louarn et al. 2000).

For generating a pointlike sodium laser guide star in the upper atmosphere at an altitude of about 90 km, one has to launch a nearly collimated laser beam with a beam diameter 2–3 times the Fried's coherence length. The optical laser beams emitted from the launching telescope toward the targeted area of obser-

---

<sup>1</sup> Subaru Telescope, National Astronomical Observatory of Japan, 650 North A'ohoku Place, Hilo, HI 96720.

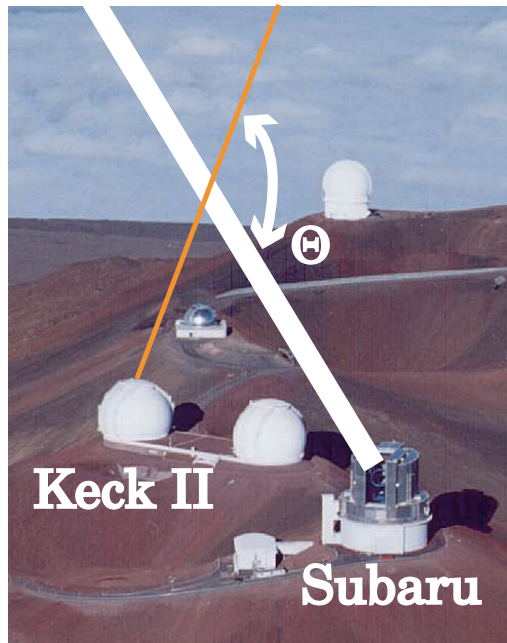


FIG. 1.—Schematic representation of the measurement configuration. The laser beam emitted from the Keck II telescope and the Subaru Telescope beam collide at a certain altitude. The parameter  $\Theta$  represents the scattering angle.

vation are actually visible to the naked eye. Thus, there is no doubt that the laser beams have a potentially disturbing effect on observations carried out with other telescopes at nearby sites, especially when the laser beam crosses their field of view.

Since there are several 8–10 m telescopes for which implementation of a sodium laser guide star system is underway or planned (Wizinowich et al. 1998b; Bonaccini et al. 2002; D’Orgeville et al. 2002; Hayano et al. 2003), establishing an agreed scheme for the coordinated operation of laser beam launching so as not to disturb observations at other telescopes is a pressing issue. The Mauna Kea community of laser guide star AO systems developers has started to organize a technical working group to establish practical rules on these issues (Wizinowich et al. 1998a). The laser beam traffic control system (LTCS), which prevents the laser beam from crossing the fields of view of other telescopes, has been proposed and implemented (Summers et al. 2003). Furthermore, additional important issue of laser safety for overhead air traffic and satellites are discussed in the working group (Wizinowich et al. 1998a).

Ageorges et al. (2000) evaluated that total magnitude of the Rayleigh scattered light from the stratosphere around 35 km altitude was 13–14 mag for a 1 W sodium laser. However, so far there was no quantitative measurement available for assessing the flux of laser light scattered at low altitude, seen from other nearby telescopes.

This paper presents the surface brightness of scattered light from the Keck II laser beam measured by the Subaru Telescope

TABLE 1  
OBSERVATION PARAMETERS FOR THE THREE COLLISIONS

Collision	Start Time (HST)	End Time (HST)	Elevation (deg)	Azimuth (deg)
1	4:47:45	5:02:30	45.0	72.0
2	5:12:55	5:21:14	60.0	76.5
3	5:38:01	5:47:06	60.0	71.0

in § 2 and discusses the possible impact on observations by other telescopes on the Mauna Kea site in § 3. The summary is given in § 4.

## 2. MEASUREMENTS AND RESULTS

The Keck II laser beam launching experiments were carried out on the nights of December 22 and 23, Hawaiian Standard Time (HST), 2001. The laser power at the launching telescope was about 17 W, and the beam waist size was about 48 cm in diameter.

The Subaru Telescope was pointed in advance to a fixed direction along the predicted Keck II laser beam tracking path, which was following a position 70" north of the star SAO 99809. We caught the Keck II laser beam in our telescope field of view before the dawn of December 24 (HST) and measured the scattered light from the laser beam. A schematic picture of the measurement configuration is shown in Figure 1. The parameter  $\Theta$  is the angle between the Keck II laser beam and the line of sight of the Subaru Telescope pointing. The observing log of the three measurements undertaken is given in Table 1.

Figure 2 presents the optical layout of the measurement system. We measured the flux of scattered laser light at the telescope pupil using the curvature wave-front sensor of the Subaru AO system (Takami et al. 2003; Gaessler et al. 2003). The field stop located at the telescope focal plane in the wave-front sensor restricts the field of view (FOV) to 5" in diameter. While the scattered light at the telescope focal plane is extremely defocused, only the incident scattered light whose direction is within that FOV is detected. Each avalanche photodiode (APD) signal indicates the flux within the corresponding subaperture of the telescope pupil. For this measurement, the telescope entrance pupil is imaged on the microlens array.

For a laser beam of diameter  $d$  with a silk-hat-like beam profile, measured at a distance  $L$  from an observing telescope with an FOV  $\theta$ , and given the magnification ratio of the pupil size at the conjugated pupil  $f'/f$ , the width of the area of the lens array illuminated by the scattered light from the laser beam is  $(d + L\theta)f'/f$ . On the other hand, the image size of the telescope aperture produced on the lens array is  $Df'/f$  for a given telescope diameter  $D$ . Thus, the scattered laser light entirely illuminates the reimaged telescope pupil only when  $d + L\theta \geq D$ . For our measurement setup with  $d = 48$  cm,  $D = 8$  m, and  $\theta = 5''$ ,  $L$  must be larger than 320 km to fill the entire telescope aperture with the scattered laser light, which is far beyond the laser guide star altitude. Therefore, it must be pointed out that, with our

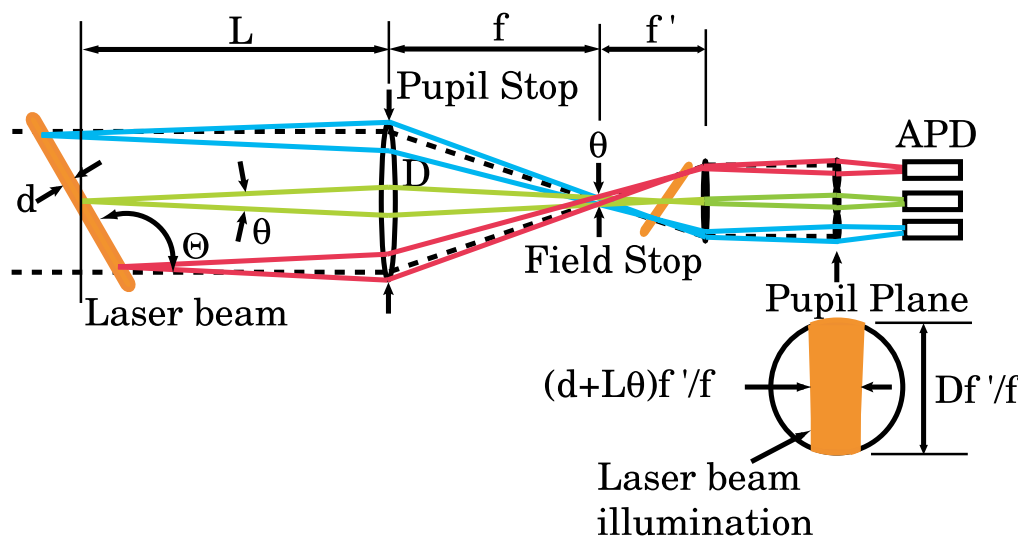


FIG. 2.—Simplified conceptual view of the setup for measuring the scattered light from the laser beam at the pupil plane. The APDs are those of the curvature wave-front sensor of the Subaru AO system. We put the field stop with the diameter of  $\theta = 5''$  at the focal plane of the curvature wave-front sensor. It means that we restrict the solid angle of scattered light by the field stop. Thus, the scattered light emitted from the laser beam cannot illuminate the whole reimaged telescope pupil in a diameter of  $Df'/f$ , but it illuminates with the width of  $(d + L\theta)f'/f$ .

measurement configuration, the scattered laser light illuminates only a small fraction of the reimaged entrance pupil. The illuminated region on the pupil has an area of  $D(d + L\theta)(f'/f)^2$ .

Next we estimate the total flux at the pupil plane. Since all the scattered light from the laser beam within the solid angle of FOV of our measuring setup is collected by the telescope of diameter  $D$ , the total flux can be estimated as  $N_{\text{ph}}(\Theta)\pi(d/2)^2(D/\sin\Theta)[\pi(\theta/2)^2/4\pi]$ , where  $N_{\text{ph}}(\Theta)$  is the number of scattered photons from the unit volume toward the angle of  $\Theta$  per unit solid angle and  $\pi(d/2)^2(D/\sin\Theta)$  represents the total volume of the laser beam, which is overlapped with the telescope beam. This formula is valid when the scattered light illuminates only the fraction of the reimaged telescope pupil due to the restricted FOV, such as our curvature wave-front sensor.

From the above considerations, we can derive the important result that the effect of scattered light from the laser beam is relatively less for a larger telescope. This is because the flux of the scattered laser light is proportional to the telescope diameter  $D$ , while the sky background is proportional to the square of the telescope diameter  $D^2$ . Thus, the ratio of scattered laser light to the sky background has a  $1/D$  dependence.

The practical impact of scattered light from a laser beam on the observing instruments mounted on other telescopes should be evaluated at their focal plane rather than at their pupil plane. Figure 3 illustrates the optical layout for a measurement at the focal plane of the telescope. The image of the scattered light from a small element of the laser beam with a diameter of  $\delta x$  located at a finite distance is usually out of focus on the instrument focal plane and has a size of  $(D + \delta x)/L \approx D/L$  (in

radians). The laser beam is observed as having the angle of  $d/L$  from the telescope, so the width of the laser beam at the telescope focal plane is  $(D + d)/L$ . For instance, the out-of-focus image size of a laser guide star at a distance of 90 km will be  $19''$ , and the corresponding size of the laser beam at 30 km would extend to  $57''$ . In the case of our measurement, the distance to the Keck II laser beam from the Subaru Telescope is typically 400 m. Thus, the laser beam subtends an angle of  $1.92$  and hence as a first approximation can be seen as an increase in the sky background.

The surface brightness at the telescope focal plane can be estimated by evaluating the flux within the area of  $1 \text{ arcsec}^2$  at the focal plane. The detailed consideration in Appendix A4 shows that the surface brightness at the telescope focal plane is equivalent to the total flux at the reimaged pupil plane, which passes through the field stop of  $1 \text{ arcsec}^2$  at the telescope focal plane. Therefore, the estimated total flux at the pupil normalized by  $1 \text{ arcsec}^2$  using our curvature wave-front sensor with  $5''$  FOV can be interpreted as the surface brightness at the telescope focal plane.

After correction for APD dark counts, the total APD counts at the telescope pupil were found to be on the order of 2000 counts  $\text{s}^{-1} \text{ arcsec}^{-2}$  at most. This value is converted to an equivalent surface brightness as  $19.5 \text{ mag arcsec}^{-2}$ , using a coefficient calibrated by the relation between APD counts and AO natural guide star  $R$ -band magnitude. The time profiles of the total flux received at the telescope pupil for the three events of beam collision are shown in Figure 4. The light curve shows two maxima and one minimum. The minimum is explained by vignetting from the Subaru secondary mirror. The measured

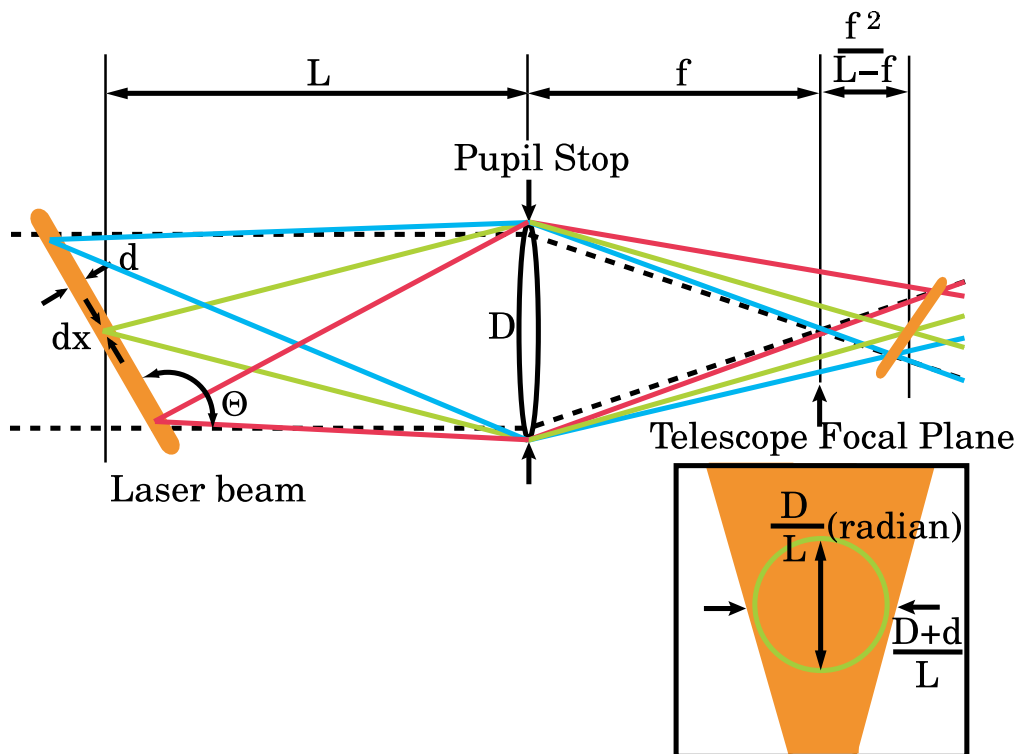


FIG. 3.—Simplified conceptual view of the setup for measuring the scattered light from the laser beam at the telescope focal plane. Consider a small element of laser beam of diameter  $\delta x$ . The diameter of this beam elements at the telescope focal plane is  $(D + \delta x)/L \approx D/L$ , where  $D$  is the telescope diameter. The flux at the telescope focal plane due to the small element is proportional to the solid angle of the scattered light expressed as  $D^2/16L^2$ , which the telescope can capture. The surface brightness due to the small element, which can be calculated by normalizing the flux by the area of the reimaged beam elements  $(D/L)^2$ , is independent of both  $D$  and  $L$ . In order to obtain the surface brightness contributed by the scattered laser light, we should integrate over the laser beam overlapped with the telescope beam. Finally, the surface brightness at the telescope focal plane is proportional to  $Dd/\sin \theta$ , if  $D \gg d$  such as for an 8 m class telescope. Thus, the surface brightness increases by  $D$ , while the sky background increases by  $D^2$ .

sky background around  $20.4 \text{ mag arcsec}^{-2}$  is consistent with the APD sensitivity spectrum and the sky background at Mauna Kea, which is summarized on-line.<sup>2</sup>

The measured APD counts when the scattered light illuminates the center of the telescope pupil are shown in Table 2. In addition, Table 2 shows the corresponding theoretically expected APD counts for the Rayleigh scattering and the Mie scattering from the Keck II laser beam evaluated by using the method described in the Appendix. The total throughput of the telescope and wave-front sensor is 0.15, as derived from standard-star observation. The model evaluation and the actual measurement agree within a factor of 2. The contribution of Mie scatter is far less than that of Rayleigh scatter because of the extremely low density of aerosols at the Mauna Kea site, e.g., less than 1/10 the value at sea level.

### 3. DISCUSSION

The scattering light of the laser beam received at the entrance aperture of the telescope through a field stop at the focal plane was evaluated in the previous section. It might be worth pointing out that despite the perceived naked-eye brightness of the sodium laser beam at the relatively low altitude of a few hundred meters, the actual measured surface brightness of the scattered beam was confirmed to be fairly modest at  $19.5 \text{ mag arcsec}^{-2}$ . The total APD counts of the Subaru AO wave-front sensor due to the sky background about  $30^\circ$  away from the full moon had been measured to be about  $19.1 \text{ mag arcsec}^{-2}$  at the commissioning observation. Using a model of a sky background as a function of separation angle from the full moon (Krisciunas & Schaefer 1991), we find that the measured flux of the scattered light from the laser beam is comparable to that of the sky background at about  $45^\circ$  away from the full moon.

Figure 5 illustrates the calculated surface brightness of both the scattered light from the laser beam and the sky background

<sup>2</sup> Available at <http://www.gemini.edu/sciops/ObsProcess/obsConstraints/ocSkyBackground.html>.

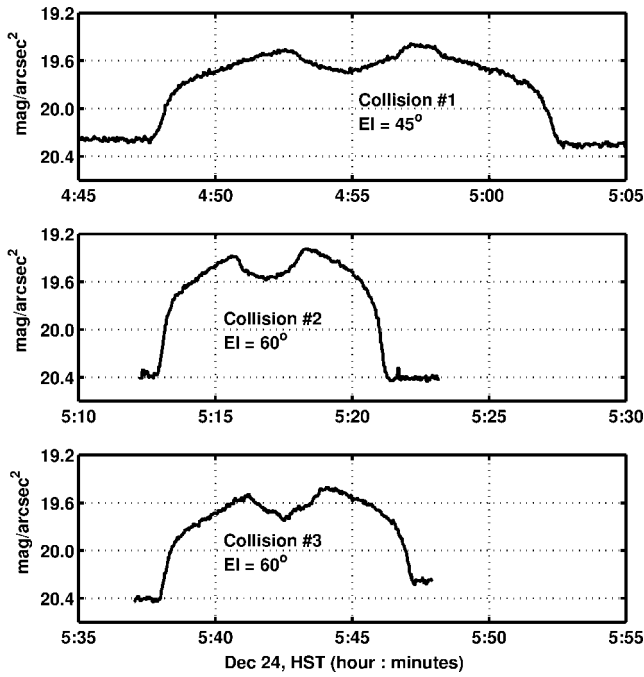


FIG. 4.—Measured surface brightness profiles of the scattered light during three observed transits of the Keck II laser beam. We estimated the surface brightness of the scattered light by calculating the total flux at the pupil plane normalized by the area size of the field stop. This is equivalent to the surface brightness at the telescope focal plane, as we explained in the discussion section. While the sky background is about 20.4 mag arcsec<sup>-2</sup>, the surface brightness increases about 19.5 mag arcsec<sup>-2</sup> when the laser beam collides with the Subaru Telescope beam. The dip in the middle of the light curve is due to the vignetting of the secondary mirror.

plotted as a function of the altitude of the scattering position. The parameters of beam collisions in calculating the surface brightness are identical to those of the measured three collisions listed in Table 2. We ignored the extinction effect of the laser beam by the atmosphere, since the total transparency of the atmosphere is about 0.85. The dot-dashed line, dashed line, and solid line represent the first, second, and third collisions, respectively. The results of our measurement are also shown in Figure 5. The symbols (*square, circle, and triangle*) correspond to each collision, sequentially. While the scattering coefficient decreases with altitude, the length of the laser beam

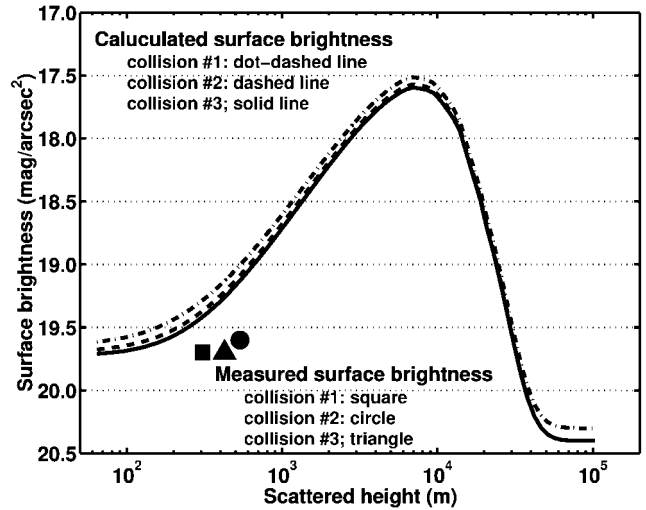


FIG. 5.—Calculated surface brightness contributed by both the scattered light from the laser beam and the sky background is plotted as a function of the altitude in the case of three collisions of Keck II and Subaru. We assume a total measurement throughput of 0.15. The dot-dashed line, dashed line, and solid line represent the first, second, and third collision, respectively. The results of our measurement are also shown. The square, circle, and triangle correspond to the results of our measurement for each collision, sequentially. The surface brightness has a peak at the collision altitude around 8 km. The surface brightness depends on the scattering coefficient and the length of the laser beam overlapped with the Subaru Telescope beam. The scattering coefficient decreases at the higher altitude, while the length of the overlapped laser beam becomes longer.

seen in the telescope field of view increases. Thus, the surface brightness takes the maximum value at an altitude of around 8 km, and its surface brightness is about 17.5 mag arcsec<sup>-2</sup>. Since the distance over which the laser beam propagates increases with increasing zenith angle, the maximum surface brightness also increases with increasing zenith angle.

However, the surface brightness exceeds 18 mag arcsec<sup>-2</sup> only when the scattered take place at a relatively high altitude between 2 and 10 km. In this case, the separation angle between the laser guide star and the telescope pointing is less than a few degrees for an observing telescope located near the laser launching telescope. Thus, the probability of causing a sub-

TABLE 2  
COMPARISON OF MEASURED AND CALCULATED APD COUNTS

Parameter	Collision 1	Collision 2	Collision 3
Elevation angle (deg) .....	45.0	60.0	60.0
Azimuth angle (deg) .....	72.0	76.5	71.0
Scattered angle $\Theta$ (deg) .....	150	159	153
Polarization angle $\alpha$ (deg) .....	77	85	104
Measured APD counts by laser (counts s <sup>-1</sup> arcsec <sup>-2</sup> ) .....	730	1000	750
Calculated APD counts (counts s <sup>-1</sup> arcsec <sup>-2</sup> ) .....	1520	2110	1660
Rayleigh scatter .....	1320	1840	1450
Mie scatter .....	200	270	210

stantial impact by the scattered light from the laser beam on general observation would be small.

Figure 6 shows the surface brightness of Keck II laser beam observed by other telescopes at Mauna Kea calculated for the case corresponding to the first collision of our measurement. Every curve has a similar shape to what one can see in Figure 5. As we mentioned in the previous section, the surface brightness measured by the smaller telescopes is larger because of the filling factor effect of the scattered light from the laser beam in the telescope aperture.

In order to estimate the scattered light from the projected laser beam in real time, further investigation using the real-time data provided with the AERONET is encouraged. For instance, the aerosol data just before dusk may well be used for independent evaluation of the scattered light from the laser beam. AERONET data acquisition relies on sunlight, but a similar method using moonlight may be useful to assess the aerosol properties during nighttime, if we can improve the sensitivity of detectors in the measuring system. In addition, the AERONET database provides the atmospheric optical thickness so that we can estimate the air mass directly. Thus, it is possible to forecast the photometric night by daytime AERONET observation. Implementing a facility for enabling AERONET measurement at Mauna Kea may also be worthy of consideration by the astronomical community.

The prediction of quantitative scattered light would allow a more flexible operation of the LTCS. The collision duration increases and the scattered laser light brightens when both telescopes are pointed in similar directions and the beams collide at high altitude. In such a case, usage of the laser would be disallowed.

On the other hand, the collision of two telescope beams at low altitude can occur only when the telescopes are pointed to very different directions. In this case, the scattered laser light is not very bright, and the collision is of short duration. For example, an observation using infrared camera and spectroscopy may even allow crossing of the laser beam and the line of sight of adjacent telescopes, because the laser beam does not affect either infrared observations or autoguiders, which use a relatively bright star to track the telescope.

Consequently, the operable probability of the laser guide star AO system could be higher than expected. Apparently, however, simultaneous observations of a common target object by laser guide star AO system on one telescope and by other nearby telescope would cause serious interference to the latter.

#### 4. CONCLUSION

We found that the surface brightness of the scattered light component at several hundred meters' height above the Keck II laser beam measured at the Subaru site was about 19.5 mag arcsec<sup>-2</sup>. The measured flux was found to be consistent within a factor of 2 with that expected for Rayleigh scattering from

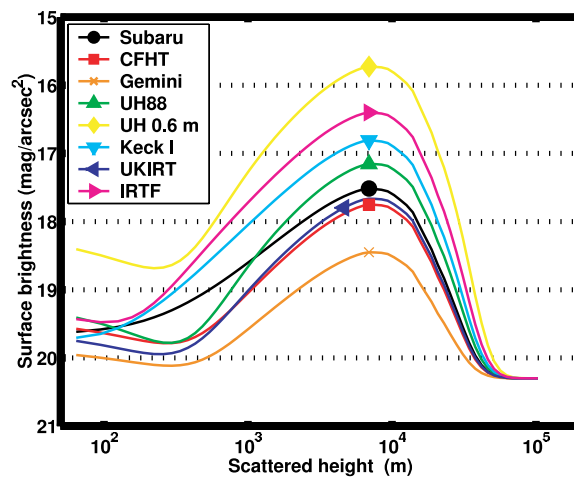


FIG. 6.—Calculated surface brightness of other telescopes at Mauna Kea in the case of the first collision of our measurement. The surface brightness becomes larger when the telescope diameter is smaller. This is because that the surface brightness increases linearly with the telescope diameter while the sky background increases by the square of telescope diameter. Also, the surface brightness becomes larger for the closer telescope from Keck II, because the overlapped laser beam with the telescope beam is getting longer.

molecules of the atmosphere plus that expected for Mie scattering based on the AERONET database.

Thus, it appears that the scattered light from such a low atmosphere is not much brighter than the sky background 45° away from the full moon. The a priori concern that scattered light from the laser beacon could be a menace for astronomical observations at adjacent telescopes may actually be unfounded. Some types of observations may well be allowed even with the crossing of the laser beam and the line of sight of the adjacent telescopes. On the other hand, the scattered light at high altitudes of around 8 km is roughly 10 times brighter than the scattered light in the lower atmosphere. However, the probability for such a collision is very small, because it occurs when the two telescopes are pointed in almost identical directions. We suggest that a flexible operation of the LTCS may increase the probability of observing with a laser guide star AO system by taking into account a quantitative prediction of scattered light.

We thank Dr. B. Holben for his effort in establishing and maintaining the Mauna Loa site of the AERONET. Suggestions on the aerosol properties and the AERONET database by Dr. M. Yasui of the Communications Research Laboratory are extremely useful and greatly appreciated. We also thank the Subaru Telescope staff, especially Messrs. Y. Mikami and A. Miyashita, for providing us with the meteorological and the particle counter data. The authors acknowledge Dr. S. Oya and Dr. D. Saint-Jacques for useful comments and fruitful discussions. In the end, we thank the anonymous referee for useful

comments and a detailed report of evaluating the surface brightness of scattered light from the laser beam at the telescope focal plane.

## APPENDIX A SCATTERED LIGHT ESTIMATION

The laser beam can be scattered mainly by molecules (Rayleigh scattering) and by aerosols (Mie scattering) in the atmosphere.

### A1. RAYLEIGH SCATTER

Rayleigh scattering in the atmosphere is well formulated (e.g., Penndorf 1957; Chandrasekhar 1950). The flux of scattered light is expressed as

$$I_R(\Theta) = \beta_R(\Theta)E, \quad (\text{A1})$$

where  $E$  is the flux of incident light and  $\beta_R(\Theta)$  is the volume angular scattering coefficient, which itself can be expressed as

$$\beta_R(\Theta) = \frac{2\pi^2(n^2 - 1)^2}{3\lambda^4 N} \frac{6 + 3p_n}{6 - 7p_n} P_R(\cos \Theta), \quad (\text{A2})$$

where  $n$  is the refractive index,  $N$  is the number density of molecules, and  $p_n = 0.035$  represents the depolarization factor of the atmosphere. The phase function  $P_R(\cos \Theta)$  expresses the angular dependence of scattering. For unpolarized incident light, the following equation can be used (Chandrasekhar 1950):

$$P_R(\cos \Theta) = \frac{3}{4(1 + 2\gamma)} \{ [2\gamma + (1 - \gamma) \cos^2 \Theta] + (1 + \gamma) \}, \quad (\text{A3})$$

where  $\gamma = p_n/(2 - p_n)$ . The first term of this equation expresses the scattered-light component from the incident light,  $E_{\parallel}$ , which is parallel to the plane including the incident ray and the scattered ray. The second term represents the scattered component from the incident ray perpendicular to the plane,  $E_{\perp}$ . We can use the same formula for the circularly polarized incident light, since the two components of incident light for both unpolarized light and the circularly polarized light can be expressed as  $E_{\parallel} = E_{\perp} = E/2$ .

For linearly polarized incident light, the two components of the incident light are

$$E_{\parallel} = E(1 + \cos 2\alpha)/2, \quad (\text{A4})$$

$$E_{\perp} = E(1 - \cos 2\alpha)/2, \quad (\text{A5})$$

where  $\alpha$  is the angle between the direction of the linear polarization vector and the plane spanned by the incident and scattered rays. Thus, the phase function can be expressed as

$$P_R(\cos \Theta) = \frac{3}{4(1 + 2\gamma)} [2\gamma + (1 - \gamma) \cos^2 \Theta + (1 + \gamma) - \cos 2\alpha(1 - \gamma)(1 + \cos \Theta^2)]. \quad (\text{A6})$$

Using these formulae, one can calculate the volume angular scattering coefficient of the Rayleigh scattering from each part of the laser beam,  $\beta_R(H, \Theta)$ , by setting the values of the angle of scattering, the polarization of the incident light, and the number density of molecules at the scattering height  $H$ , which we can estimate from radiosonde observation at Hilo, the city at the foot of Mauna Kea.

The data archive of radiosonde observations is available on-line.<sup>3</sup>

<sup>3</sup> <http://weather.uwyo.edu/upperair/sounding.html>.

## A2. MIE SCATTER

The calculation of Mie scattering due to aerosol in the atmosphere, on the other hand, is not straightforward, as the amount and the size distribution of the aerosol vary with time and are not formulated by a simple model. Instead of modeling, we refer to the AERONET observation database (Holben et al. 2001), which is a network project monitoring the aerosol in various parts of the world. AERONET provides the observed data on atmospheric extinction of sunlight and the flux of the scattered sunlight, yielding an estimate of the various optical properties and size distribution of aerosols for the entire atmospheric column.

We assume that the aerosol distribution above Mauna Kea (4200 m) is equivalent to that above the Mauna Loa Observatory (3400 m), since both sites are above the usual height of the aerosol mixing layer (typically at around 2000 m). Furthermore, the humidity, wind speed, wind direction, and temperature at these two sites correlate well when one compares data from the meteorological towers of Subaru Telescope and Mauna Loa Observatory, the latter maintained by NOAA Climate Monitoring and Diagnostics Laboratory and available by ftp.<sup>4</sup> Moreover, we observed that the size distribution inferred from the particle count data measured at the Subaru site in 2001 March appears to be correlated with that derived from the AERONET observation at the Mauna Loa Observatory.

The amount of aerosol at the Mauna Loa Observatory shows a diurnal variation with general increase during the day and decrease in the evening (Perry et al. 1999). This phenomenon can be explained by the typical daytime upslope winds and nighttime downslope winds (Mendonca 1969; Perry et al. 1999). We assume that the amount of aerosol and its size distribution measured at dawn are a reasonable estimate of their nighttime values.

The volume angular scattering coefficient for Mie scatter  $\beta_M(H, \Theta)$  is required to estimate the Mie scattered light. First, the volume angular scattering coefficient of the entire atmospheric column  $\tilde{\beta}_{M_{\text{total}}}(\Theta)$  is derived from the AERONET data. This parameter  $\tilde{\beta}_{M_{\text{total}}}(\Theta)$ , which represents the contribution from the entire atmosphere to the scattered light component with a scattering angle  $\Theta$  between the incident ray and the ray scattered by an aerosol, can be derived by

$$\tilde{\beta}_{M_{\text{total}}}(\Theta) = \omega \tau_{\text{abs}} P_M(\cos \Theta) / 4\pi, \quad (\text{A7})$$

where  $\omega$  is the single scattering albedo,  $\tau_{\text{abs}}$  is the absorption coefficient for the entire atmospheric column, and  $P_M(\cos \Theta)$  is the phase function (Nakajima et al. 1996). These three parameters are provided by the AERONET database.

The AERONET database provides us with the phase function for unpolarized incident light. Thus, we have to consider the effect of polarized incident light to evaluate the scattered light from the laser beam. Generally, the phase function can be expressed by two components, perpendicular and parallel to the plane defined by the vectors of incident light and scattered light. Here the aerosol is assumed to be spherical so that there is no depolarization effect for Mie scattering. Thus, we can consider the perpendicular and parallel components independently. As we discussed above in evaluating Rayleigh scatter, the phase function of circular incident light is identical to that of unpolarized incident light, since the two components of incident light have the same relation,  $E_{\parallel} = E_{\perp} = E/2$ . Therefore, the phase function can be expressed as  $P_{M_{\text{unpol}}}(\cos \Theta) = [P_{M_{\perp}}(\cos \Theta) + P_{M_{\parallel}}(\cos \Theta)]/2$  for unit irradiance.

For linear polarized light, the incident light can be expressed by equations (A4) and (A5). The phase function becomes

$$P_{M_{\text{linpol}}}(\cos \Theta) = P_{M_{\perp}}(\cos \Theta)(1 - \cos 2\alpha)/2 + P_{M_{\parallel}}(\cos \Theta)(1 + \cos 2\alpha)/2, \quad (\text{A8})$$

$$= P_{M_{\text{unpol}}}(\cos \Theta) + \cos 2\alpha [P_{M_{\parallel}}(\cos \Theta) - P_{M_{\perp}}(\cos \Theta)]/2. \quad (\text{A9})$$

The difference between the phase function for unpolarized incident light and linear polarized incident light is attributed to the second term of the above equation. However, this second term is significant only when the scattering angle  $\Theta$  approaches  $90^\circ$  (see Deirmendjian 1969). Thus, we do not need to take the status of polarization of the incident laser beam into account for evaluating the Mie scatter in our measurement setup.

On the other hand,  $\tilde{\beta}_{M_{\text{total}}}(\Theta)$  can be expressed as

$$\tilde{\beta}_{M_{\text{total}}}(\Theta) = \int_{H_G}^{\infty} \beta_M(H_G, \Theta) \exp[-(H - H_G)/H_0] dH = \beta_M(H_G, \Theta) H_0, \quad (\text{A10})$$

where  $H_G$  is the height of the ground at the site and  $\beta_M(H_G, \Theta)$  gives the volume angular scattering coefficient at ground level. Here we assume that the vertical profile of the aerosol density decreases exponentially with a scale height  $H_0$ .

<sup>4</sup> ftp://140.172.192.211/met/hourlymet/mlo/mlo2001.

The equivalent volume angular scattering coefficient at the altitude  $H$ ,  $\beta_M(H, \Theta)$ , is therefore

$$\beta_M(H, \Theta) = (\tilde{\beta}_{M_{\text{total}}}/H_0) \exp [-(H - H_G)/H_0]. \quad (\text{A11})$$

We estimated the scale height  $H_0$  as follows. AERONET provides the distribution of the aerosol particle volume,  $d\tilde{V}(r)/d \ln r$ , integrated vertically through the atmosphere. This quantity can be written as

$$d\tilde{V}(r)/d \ln r = \frac{4\pi r^3}{3} d\tilde{N}(r)/d \ln r, \quad (\text{A12})$$

where  $d\tilde{N}(r)/d \ln r$  represents the distribution of aerosol particle number and all the particles are assumed to be spherical in shape. In addition to the AERONET measurement, we have separate data on the size distribution of particle at ground level  $[dN(r)/d \ln r]_{H_G}$  measured by the particle counter installed at the Subaru Telescope. By assuming an exponential vertical distribution of particles expressed as

$$d\tilde{N}(r)/d \ln r = \int_{H_G}^{\infty} [dN(r)/d \ln r]_{H_G} \exp [-(H - H_G)/H_0] dH, \quad (\text{A13})$$

we can derive the scale height

$$H_0 = \frac{d\tilde{N}(r)/d \ln r}{[dN(r)/d \ln r]_{H_G}}. \quad (\text{A14})$$

The analysis of the measured data from the particle counter at the Subaru Telescope and the reported AERONET data for the aerosol particle volume distribution between 2001 March 15 and April 3 reveals that the scale height is on average around 3 km.

### A3. TOTAL FLUX OF SCATTERED LIGHT OBSERVED BY THE TELESCOPE

The actual flux of the scattered light observed at the telescope can be estimated by assuming a Gaussian laser beam profile  $I_0 \exp(-2r^2/w_0^2)$  as a function of lateral displacement from the optical axis of the laser beam  $r$ , with a peak intensity  $I_0$  and a beam waist size in diameter  $2w_0$ . The total photon number per second that contributes to the scattering can be expressed as

$$N_p = \frac{2\pi \int_0^{\infty} I_0 \exp(-2r^2/w_0^2) r dr}{h\nu} z \quad (\text{A15})$$

$$= \frac{E_0}{h\nu} z, \quad (\text{A16})$$

with the length of overlapped laser beam  $z = D/\sin \Theta$ , where  $D$  is the telescope aperture diameter,  $E_0$  is the averaged total laser power,  $h$  is the Planck constant, and  $\nu$  is the frequency of the laser. The final expression for the flux of the scattered light is thus

$$F = N_p[\beta_R(H, \Theta) + \beta_M(H, \Theta)] d\Omega, \quad (\text{A17})$$

where  $d\Omega$  is the solid angle of the scattered light.

### A4. THE SURFACE BRIGHTNESS AT THE TELESCOPE FOCAL PLANE

In order to estimate the surface brightness of scattered light from the laser beam at the telescope focal plane, let the measuring setup be as shown in Figure 3. The distance to the laser beam is  $L$ , telescope diameter is  $D$ , and the focal length of the telescope is  $f$ . Consider a small element of laser beam with a volume of  $\delta x^3$ . The diameter of this beam element at the telescope focal plane is  $D/L/(4.8 \times 10^{-6})$  in arcseconds. Here we assume that  $\delta x \ll D$  and  $\delta x \ll L$ . On the other hand, we can easily calculate the solid angle of the scattered light, which the telescope can observe, as  $d\Omega = D^2/16L^2$ . The surface brightness is calculated by normalizing the area of beam element at the focal plane and by integrating over the laser beam, which is overlapped with the telescope beam.

Then we obtain it as

$$N_{\text{ph}}(\Theta)\pi(d/2)^2(D/\sin\Theta)(D^2/16L^2)/\{\pi[D/L/(4.8 \times 10^{-6})]^2\} \quad (\text{A18})$$

$$= N_{\text{ph}}(\Theta)\pi(d/2)^2(D/\sin\Theta)[(4.8 \times 10^{-6})^2/4\pi]. \quad (\text{A19})$$

where we assume  $D \gg d$ . Thus, with the condition of  $D \gg d$ , such as an 8 m class telescope, the surface brightness increases by  $D$ , while the sky background increases by  $D^2$ . Note that the formula of the surface brightness at the telescope focal plane is identical to that of the total flux at the telescope pupil in equation (A1), setting the FOV as 1 arcsec<sup>2</sup>. Therefore, the estimated total flux at the pupil normalized by 1 arcsec<sup>2</sup> using our curvature wave-front sensor with 5" FOV can be interpreted as the surface brightness at the telescope focal plane.

On the other hand, if  $D \ll d$ , such as with the naked eye or a sky monitor camera, the overlapped laser beam, which is restricted by the telescope diameter  $D$ , approximately becomes  $(Dd)(D/\sin\Theta)$ . Then the surface brightness is

$$N_{\text{ph}}(\Theta)(D^2d/\sin\Theta)[(4.8 \times 10^{-6})^2/4\pi]. \quad (\text{A20})$$

The surface brightness increases by  $D$  until the telescope diameter exceeds the laser beam diameter.

## REFERENCES

- Ageorges, N., Redfern, R. M., Delplancke, F., & O'Sullivan, C. 2000, Proc. SPIE, 4007, 384  
 Bonaccini, D., et al. 2002, Proc. SPIE, 4494, 276  
 Chandrasekhar, S. 1950, Radiative Transfer (London: Oxford Univ. Press)  
 Deirmendjian, D. 1969, Electromagnetic Scattering on Spherical Polydispersions (New York: Elsevier)  
 D'Orgeville, C., Bauman, B. J., Catone, J. W., Ellerbroek, B. L., Gave, D. T., & Buchroeder, R. A. 2002, Proc. SPIE, 4494, 302  
 Gaessler, W., Takami, H., Takato, N., Hayano, Y., Kamata, Y., Saint-Jacques, D., Minowa, Y., & Iye, M. 2003, Proc. SPIE, 4839, 954  
 Hayano, Y., et al. 2003, Proc. SPIE, 4839, 32  
 Holben, B. N., et al. 2001, J. Geophys. Res., 106, 12067  
 Krisciunas, K., & Schaefer, B. E. 1991, PASP, 103, 1033  
 Le Louarn, M., Hubin, N., Sarazin, M., & Tokovinin, A. 2000, MNRAS, 317, 535  
 Mendonca, B. G. 1969, J. Appl. Meteorol., 8, 533  
 Nakajima, T., Tonna, G., Rao, R., Boi, P., Kaufman, Y., & Holben, B. 1996, Appl. Opt., 35, 2672  
 Penndorf, R. 1957, J. Opt. Soc. Am., 47, 176  
 Perry, K. D., Cahill, T. A., Schnell, R. C., & Harris, J. M. 1999, J. Geophys. Res., 104, 18521  
 Summers, D., et al. 2003, Proc. SPIE, 4839, 440  
 Takami, H., Takato, N., Hayano, Y., Iye, M., Kamata, Y., Minowa, Y., Kanzawa, T., & Gaessler, W. 2003, Proc. SPIE, 4839, 21  
 Wizinowich, P. L., Simons, D. A., Takami, H., Veillet, C., & Wainscoat, R. J. 1998a, Proc. SPIE, 3353, 290  
 Wizinowich, P. L., et al. 1998b, Proc. SPIE, 3353, 568